

Addition of one and two units of C₂H to styrene: A theoretical study of the C₁₀H₉ and C₁₂H₉ systems and implications toward growth of polycyclic aromatic hydrocarbons at low temperatures

Alexander Landera,¹ Ralf I. Kaiser,² and Alexander M. Mebel^{1,a)}

¹*Department of Chemistry and Biochemistry, Florida International University, 11200 SW 8th Street, Miami, Florida, 33139, USA*

²*Department of Chemistry, University of Hawai'i at Manoa, Honolulu, Hawaii 96822-2275, USA*

(Received 17 September 2010; accepted 24 November 2010; published online 11 January 2011)

Various mechanisms of the formation of naphthalene and its substituted derivatives have been investigated by *ab initio* G3(MP2,CC)/B3LYP/6-311G** calculations of potential energy surfaces for the reactions of one and two C₂H additions to styrene combined with RRKM calculations of product branching ratios under single-collision conditions. The results show that for the C₂H + styrene reaction, the dominant routes are H atom eliminations from the initial adducts; C₂H addition to the vinyl side chain of styrene is predicted to produce *trans* or *cis* conformations of phenylvinylacetylene (**t**- and **c**-PVA), whereas C₂H addition to the *ortho* carbon in the ring is expected to lead to the formation of *o*-ethynylstyrene. Although various reaction channels may lead to a second ring closure and the formation of naphthalene, they are not competitive with the direct H loss channels producing PVAs and ethynylstyrenes. However, **c**-PVA and *o*-ethynylstyrene may undergo a second addition of the ethynyl radical to ultimately produce substituted naphthalene derivatives. α - and β -additions of C₂H to the side chain in **c**-PVA are calculated to form 2-ethynyl-naphthalene with branching ratios of about 30% and 96%, respectively; the major product in the case of α -addition would be *cis*-1-hexene-3,5-diynyl-benzene produced by an immediate H elimination from the initial adduct. C₂H addition to the ethynyl side chain in *o*-ethynylstyrene is predicted to lead to the formation of 1-ethynyl-naphthalene as the dominant product. The C₂H + styrene \rightarrow **t**-PVA + H/**c**-PVA + H/*o*-ethynylstyrene, C₂H + **c**-PVA \rightarrow 2-ethynyl-naphthalene + H, and C₂H + *o*-ethynylstyrene \rightarrow 1-ethynyl-naphthalene + H reactions are calculated to occur without a barrier and with high exothermicity, with all intermediates, transition states, and products lying significantly lower in energy than the initial reactants, and hence to be fast even at very low temperature conditions prevailing in Titan's atmosphere or in the interstellar medium. If styrene and C₂H are available and overlap, the sequence of two C₂H additions can result in the closure of a second aromatic ring and thus provide a viable route to the formation of 1- or 2-ethynyl-naphthalene. The analogous mechanism can be extrapolated to the low-temperature growth of polycyclic aromatic hydrocarbons (PAH) in general, as a step from a vinyl-PAH to an ethynyl-substituted PAH with an extra aromatic ring. © 2011 American Institute of Physics. [doi:10.1063/1.3526957]

I. INTRODUCTION

The present estimates place the percentage of carbon in our galaxy involved in polycyclic aromatic hydrocarbon (PAH) at between 2% and 30%.¹ The existence of PAH in the interstellar media (ISM) was suggested early on by the spectroscopic analysis of infrared radiation (IR) emission bands by Allamandola and coworkers in 1989.² Recently, a more detailed analysis of characteristic spectral bands between 15 and 20 μ m has revealed the presence of CCC out-of-plane bending vibrations likely due to PAHs.³ Moreover, based on the IR spectra from the interacting galaxy UGC 10214 (the Tadpole galaxy), it has also been suggested that extranuclear star formation is accompanied by PAH formation, further establishing the importance of PAHs in astrochemistry.⁴ In our own

Solar System, PAHs represent an important class of molecules and their production and growth processes deserve careful consideration. Although they have not been observed directly in planetary atmospheres, PAHs have been identified in laboratory experiments simulating Jupiter's atmosphere and also the atmospheric chemistry of Saturn's moon Titan.⁵ It is strongly believed that PAHs are primarily responsible for the famous orange/brownish haze layers found on Titan. Early laboratory simulations by Khare *et al.* suggested a possible existence of substituted PAHs in Titan's tholins.⁶ In 1993, again by utilizing simulated Titan atmospheres, Khare *et al.* have detected several two- to four-ring PAHs by using a two step laser desorption mass spectrometry method, but no definite chemical identification could be made.⁷ In 2002, Khare *et al.* studied the nature of laboratory simulated Titan's haze layers and ascertained, by time dependent IR and GCMS techniques, that aromatics are formed within the first few seconds of simulation.⁸ PAH precursors are also postulated to exist

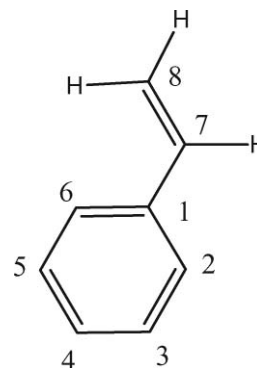
^{a)} Author to whom correspondence should be addressed. Electronic mail: mebela@fiu.edu.

in Titan's atmosphere. For instance, Coustenis and coworkers in 2003 reported the first spectroscopic identification of benzene at 674 cm^{-1} .⁹ Hard evidence for benzene on Titan was finally achieved in 2007 by using the Composite Infrared Spectrometer (CIRS) instrument on board Cassini.¹⁰ Naphthalene, the simplest PAH, has been also postulated to exist on Titan. For instance, naphthalene was detected in 2006 as one of the tholin pyrolysis products using a two-dimensional GC/MS technique.¹¹

Until recently, the kinetic models of the PAH formation and growth in low temperature environments such as on Titan or in the ISM relied upon the models of PAH and soot formation in combustion processes^{12–14} and assumed that similar mechanisms are important both at combustion temperatures (1000–2500 K) and in the extraterrestrial, low temperature environments (10–150 K).¹⁵ Wilson *et al.*^{15–17} suggested, for instance, that once the first aromatic ring is available, the further growth of PAHs proceeds by the hydrogen-abstraction-acetylene-addition (HACA) mechanism, which is believed to be the most important PAH formation mechanism in combustion flames.¹² However, an apparent flaw of these models is that both hydrogen abstraction and acetylene addition reactions exhibit significant barriers and as a result are very slow at low temperatures relevant to the atmospheric conditions on Titan or in the ISM. As a low-temperature alternative to HACA, we have recently proposed a new ethynyl addition mechanism (EAM) of PAH growth.¹⁸ Within EAM, an addition of the ethynyl radical C_2H to benzene, produces phenylacetylene $\text{C}_6\text{H}_5\text{C}_2\text{H}$ after H loss from the initial adduct. Next, a second C_2H addition to the *ortho* carbon atom of phenylacetylene gives a reaction intermediate, which then rapidly loses a hydrogen atom forming 1,2-diethynylbenzene. The latter can react with a third ethynyl molecule via addition to a carbon atom of one of the ethynyl side chains and a consecutive ring closure of the intermediate leads to an ethynyl-substituted naphthalene core. Under single collision conditions of the ISM, this core loses a hydrogen atom to form ethynyl-substituted 1,2-didehydronaphthalene, but under higher pressures of Titan's atmosphere, three-body reactions can lead to a stabilization of this naphthalene-core intermediate. The reactions of C_2H and C_2H -like radicals with a variety of unsaturated and aromatic hydrocarbons have been shown to be fast, with rate constants in the order of $10^{-10}\text{ cm}^3\text{ molecule}^{-1}\text{ s}^{-1}$, both experimentally and theoretically even at temperatures down to 15 K (Refs. 19–23) and hence, the viability of EAM would depend on the abundance of the reactant species. On Titan, the ethynyl radical can be produced easily by the photolysis of acetylene.^{24–27} However, a drawback of the EAM involving benzene is that it can only produce dehydronaphthalene derivatives and then H (or a hydrocarbon radical) additions followed by collisional or radiative stabilization are required to form closed-shell PAH molecules.¹⁸

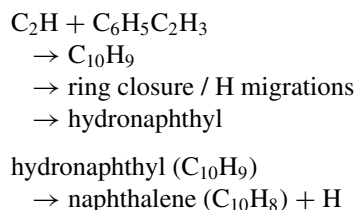
In view of this deficiency of the $\text{C}_2\text{H}/\text{C}_6\text{H}_6$ EAM, in the present work we consider a possibility of naphthalene formation via consecutive additions of ethynyl radicals to styrene, $\text{C}_6\text{H}_5\text{C}_2\text{H}_3$ (C_8H_8).

A recent laboratory simulation of tholin production by Pietrogrande and coworkers suggests that styrene may be present on Titan.²⁸ This finding was also confirmed by a di-



SCHEME 1. Structure and atom numbering system of styrene.

rect analysis of differentially irradiated Titan-like gas samples by Ramirez *et al.*²⁹ Furthermore, Kaiser's group has shown, by crossed molecular beam experiments, that in combustion flames, styrene can be formed by the addition of ethylene to phenyl radical.³⁰ The addition of ethynyl radical to styrene may offer a possible route to the formation of naphthalene. Styrene (see Scheme 1) has two principal carbons which may be attacked by C_2H (labeled "6" and "8") with a possibility of subsequent ring closure followed by H elimination leading to the formation of naphthalene via the following reaction sequence:



To investigate these possibilities, in the present work we describe potential energy surfaces (PES) for the reactions of addition of one and two C_2H units to styrene and determine whether naphthalene or any of its derivatives can be formed in these reactions in the cold temperature environments of Titan or ISM. This study is performed through detailed and chemically accurate calculations of various intermediates, transition states (TS), and products on each PES. Rate constants for various unimolecular reaction steps are then computed using Rice-Ramsperger-Kassel-Marcus (RRKM) theory and finally, product branching ratios are evaluated depending on the collision energy.

II. COMPUTATIONAL METHODS

All stationary points, including isomers, products, and TS, were optimized using the hybrid density functional B3LYP³¹ method with the split-valence Pople's 6-311G** basis set. Frequencies and zero point energies (ZPE) were also computed at the same level of theory. All B3LYP energies were further refined using the G3(MP2,CC) modification³² of the original Gaussian 3 (G3) scheme.³³ The final energies at 0 K were obtained using the B3LYP optimized geometries and ZPE corrections according to the following formula:

$$E[\text{G3}(\text{MP2,CC})] = E[\text{CCSD}(\text{T})/6\text{-311G}(d,p)] + \Delta E_{\text{MP2}} + E(\text{ZPE}).$$

Here ΔE_{MP2} is the basis set correction, formally, $E[\text{MP2}/\text{G3Large}] - E[\text{MP2}/6\text{-}311\text{G}(d,p)]$. $\Delta E(\text{SO})$, the spin-orbit correction, and $\Delta E(\text{HLC})$, the higher level correction, from the original G3 scheme were not included in our calculations, as they are not expected to make significant contributions into relative energies. Geometric optimizations, frequency calculations, and MP2 calculations were all performed using the GAUSSIAN 98 and 09 quantum chemistry package,^{34,35} whereas all spin-restricted coupled cluster RCCSD(T) calculations were performed using the MOLPRO program.³⁶ All optimized Cartesian coordinates, energetic and molecular parameters, including rotational constants and vibrational frequencies, of various structures can be found in Table S1 of supplementary material.³⁷

Rate constants of individual unimolecular reactions under single-collision conditions were evaluated within RRKM theory.³⁸ We calculated rate constants as functions of available internal energy of each intermediate or transition state; the internal energy was taken as the energy of chemical activation in each reaction plus collision energy. Only a single total energy level was considered throughout, as for single-collision conditions (zero-pressure limit). The harmonic approximation was used in calculations of numbers and densities of states needed to evaluate the rate constants. The calculated rate constants are collected in Table S2 of supplementary material.³⁷ It should be noted that no variational RRKM calculations were required for the systems considered in this work, because all significant reaction channels, including those for H eliminations proceeding via relatively “loose” transition states, exhibit distinct barriers of at least 2–3 kcal/mol in both forward and reverse directions. In our experience, when such distinct barriers exist, variational treatment of the transition state does not alter the calculated rate constant significantly as compared to the conventional “constrained” transition state analysis.

With all unimolecular rate constants in hand, we solved first-order phenomenological rate equations to determine product branching ratios for the decomposition of chemically activated initial adducts of the first and second C₂H addition to styrene. We utilized a universal computer code developed earlier by our group³⁹ for an arbitrary first-order reaction system, which employs the fourth-order Runge–Kutta method to obtain numerical solutions for the concentrations of various products versus time. The concentrations at the times when they have converged are used for calculations of the product branching ratios. In addition, our code can also use the steady-state approximation to compute the branching ratios. The steady-state expressions for the rates of formation for all significant products are given in the supplementary material.³⁷ The accuracy of the G3(MP2) method employed in this paper for the calculations of relative energies is normally within 1–2 kcal/mol.^{32,33} As will be shown below, for all considered reactions, except for the H loss from **i1** and **i2**, the critical barriers are separated by at least 8 kcal/mol, implying that the competitive barriers are well resolved and that there should be relatively little sensitivity of the computed product branching ratios with respect to the expected errors in computed barrier heights.

III. RESULTS AND DISCUSSION

A. C₂H + styrene reaction channels

The reaction of C₂H radical with styrene at the eighth position occurs without a barrier, and forms **i1** and **i2**, with exothermicity of 63.9 and 63.2 kcal/mol, respectively. As seen in Fig. 1, **i1** and **i2** are conformational isomers produced in the entrance channels and should be able to easily interconvert to each other by rotation around a single C–C bond, which is expected to have a low barrier. **i1** is capable of pursuing three distinct reaction paths. The first one,

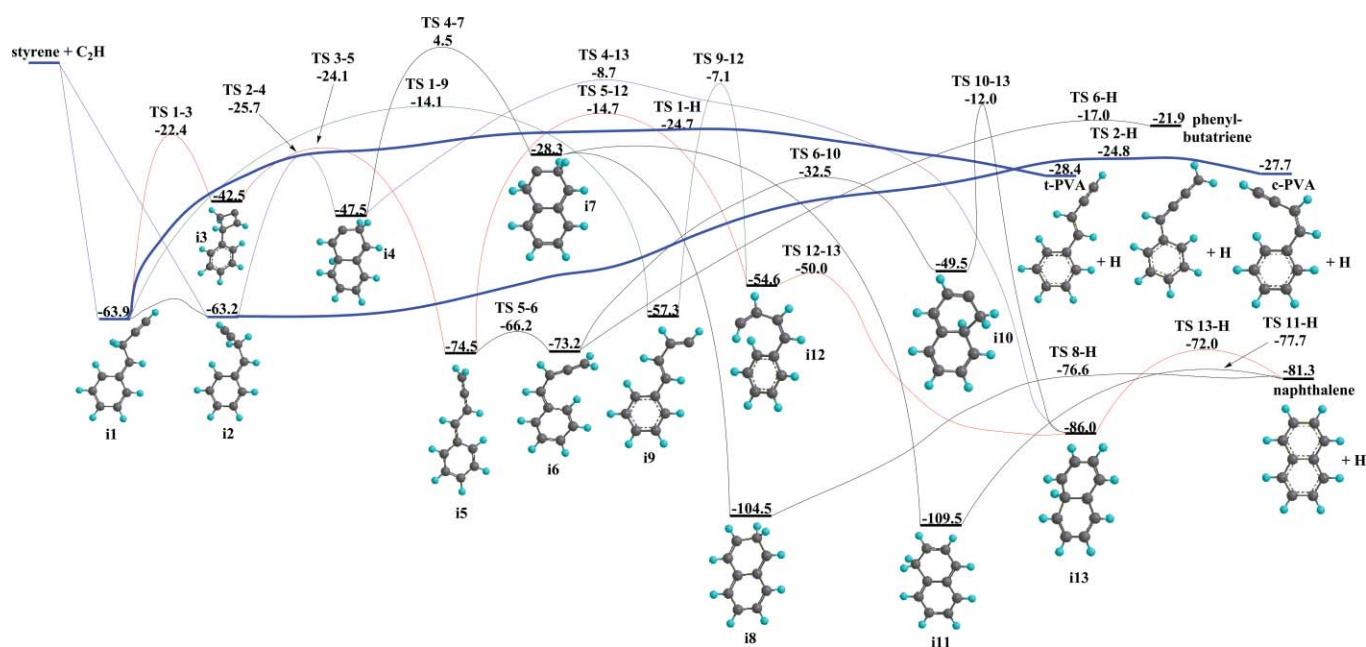


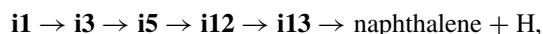
FIG. 1. Potential energy diagram of the styrene + C₂H reaction (channels initiated by the C₂H addition to the C⁸ atom in styrene) calculated at the G3(MP2,CC)//B3LYP/6-311G** + ZPE(B3LYP/6-311G**) level of theory. All relative energies are given in kcal/mol with respect to the initial reactants.



involves loss of a hydrogen atom from the tetrahedral carbon center 8 and leads to **t-PVA** lying 28.4 kcal/mol lower in energy than the initial reactant species. The reaction has an activation barrier of 39.2 kcal/mol with the corresponding transition state at -24.7 kcal/mol relative to the reactants. In an alternative channel,



i1 can migrate a hydrogen atom, again from its tetrahedral carbon center, to an adjacent hydrogen-free carbon to create **i9**. Rotation around a side-chain double bond in **i9** produces another isomer **i12**. Next, **i12** can readily cyclize proceeding to **i13**, 9-H-naphthyl radical. **i13** can promptly lose a hydrogen atom forming naphthalene as the final product. The highest in energy transition state on the $\text{C}_2\text{H} + \text{styrene} \rightarrow \mathbf{i1} \rightarrow \mathbf{i9} \rightarrow \mathbf{i12} \rightarrow \mathbf{i13} \rightarrow \text{naphthalene} + \text{H}$ pathway is TS 9–12 residing 7.1 kcal/mol below the initial reactants. However, TS 9–12 is 17.6 kcal/mol higher in energy than TS 1-H, the transition state for the direct H loss from **i1**. The third alternative channel,

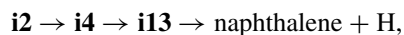


proceeds from **i1** to the bicyclic compound **i3**, which lies at a relative energy of -42.5 kcal/mol. Ring opening in **i3** forms **i5** with a relative energy of -74.5 kcal/mol. 1,2-Hydrogen migration from the terminal CH_2 group in **i5** via a barrier located at -14.7 kcal/mol can lead to **i12**, which then can isomerize to **i13** and then dissociate to naphthalene + H. **i5** can also rearrange to **i6** through a simple single bond rotation. Next, a ring closure may occur via a barrier positioned at -32.5 kcal/mol to form **i10**, which in turn can interconvert to **i13** by hydrogen migration via a barrier located at -12.0 kcal/mol and **i13** can then readily form naphthalene. Otherwise, a direct hydrogen loss from **i6**, which proceeds via a barrier located at -17.0 kcal/mol, can lead to phenylbutatriene.

Now we turn our attention to the second initial intermediate **i2**. A direct hydrogen loss from **i2** can form *cis*-phenylvinylacetylene (**c-PVA**),



To do so, **i2** needs to overcome an energy barrier located at -24.8 kcal/mol relative to the initial reactants. In the other channel,



i2 may cyclize via a barrier at -25.7 kcal/mol to form **i4**, which has a relative energy of -47.5 kcal/mol. Hydrogen migration from the CH_2 group in the newly formed second ring of **i4** can lead to **i13**, via a transition state positioned at -8.7 kcal/mol, and **i13** then can directly proceed to naphthalene. 1,2-Hydrogen migration may also occur from the carbon atom of the C–C bond common for the two rings in **i4** producing **i7**. However, in this case the barrier is much higher, with the corresponding transition state lying 4.5 kcal/mol above the initial reactants. Next, two different hydrogen shifts (from two CH_2 groups in **i7** to the adjacent hydrogen-less carbon

atom between them) can produce **i8** and **i11**. We were able to locate transition states for $\mathbf{i7} \rightarrow \mathbf{i8}$ and $\mathbf{i7} \rightarrow \mathbf{i11}$ at the B3LYP level and the calculations show that the corresponding barriers were very low. Single-point G3(MP2,CC) calculations gave energies of these TSs slightly lower than that of **i7**. This result indicates that **i7**, if exists, can represent only a metastable local minimum; once the H migration via TS 4–7 is completed, both **i8** and **i11** can be immediately produced. **i8** and **i11** reside in very deep potential wells and can be described as 2-hydro- and 1-hydronaphthyl radicals, respectively. H elimination from the CH_2 groups in **i8** and **i11** finally lead to naphthalene via barriers at -76.6 and -77.7 kcal/mol, respectively.

In order to understand what products can be formed in the $\text{C}_2\text{H} + \text{styrene}$ reaction channels shown in Fig. 1, we employed RRKM theory to compute unimolecular rate constants for dissociation and isomerization of the C_{10}H_9 intermediates formed after barrierless addition of ethynyl radical to styrene under single-collision conditions and the collision energy ranging from 0 to 5 kcal/mol. Then the rate constants were used to solve first-order kinetic equations and to calculate product branching ratios. These calculations show that when C_2H adds to position 8 initially forming **i1** or **i2** (Fig. 1), **t-PVA** and **c-PVA** are expected to be nearly exclusive reaction products. The direct H loss from **i1/i2** is favored both by lower barriers and looser transition states. For instance, the H loss barriers are ~ 39 kcal/mol, whereas the highest barrier on the most favorable $\mathbf{i1} \rightarrow \mathbf{i3} \rightarrow \mathbf{i5} \rightarrow \mathbf{i12} \rightarrow \mathbf{i13}$ cyclization pathway occurring at TS 5–12 is ~ 49 kcal/mol relative to **i1**, i.e., around 10 kcal/mol higher. A comparison of the rate constants of the competing initial reaction steps, $\mathbf{i1} \rightarrow \textit{t-PVA} + \text{H}$, $\mathbf{i1} \rightarrow \mathbf{i3}$, and $\mathbf{i1} \rightarrow \mathbf{i9}$ (5.20×10^4 , 7.70×10^2 , and $8.07 \times 10^0 \text{ s}^{-1}$ at zero collision energy, respectively, see Table S2), as well as $\mathbf{i2} \rightarrow \textit{c-PVA} + \text{H}$ and $\mathbf{i2} \rightarrow \mathbf{i4}$ (2.60×10^4 and $1.90 \times 10^3 \text{ s}^{-1}$, respectively), clearly confirms the preference of the direct H loss from **i1/i2** over the isomerization processes. Since **i1** and **i2** should rapidly equilibrate, the rate constant for the formation of **c-PVA** + H from **i1** in our kinetic calculations can be evaluated as $k_{1-2}/k_{2-1}k_{2-H}$. The k_{1-2}/k_{2-1} ratio is the equilibrium constant between **i1** and **i2**, which can be computed as a ratio of the densities of states of **i1** and **i2** at a given internal energy. Therefore, the $k_{1-2}/k_{2-1}k_{2-H}$ value can be calculated as a RRKM rate constant for a process in which **i1** is the reactant and TS 2-H is the transition state. Such calculations give the value of $2.19 \times 10^4 \text{ s}^{-1}$ for $\mathbf{i1} \rightarrow \textit{c-PVA} + \text{H}$ at zero collision energy (Table S2) and result in the **t-PVA/c-PVA** branching ratios of 2.4–2.5:1 for collision energies in the 0–5 kcal/mol range. However, since the energies of the **i1** and **i2** adducts and their corresponding H loss transition states are close, this result is likely to be sensitive to the accuracy of *ab initio* calculations. The computed branching ratios of all other products, including naphthalene and phenylbutatriene are negligible.

An important issue, which needs to be addressed here, is a possibility of collisional stabilization of **i1/i2** in the PAH forming region of Titan's atmosphere. According to Wilson and Atreya,¹⁵ such region on Titan spans from approximately 140 to 300 km above the surface, with the peak PAH production occurring at about 220 km. Liang *et al.*⁴⁰ suggested that haze formation takes place in the 300–500 km region. In

any case, while the pressure at the surface of Titan is about 1.5 bar, the atmospherically relevant pressure window in the PAH forming region is 1 to 10⁻⁶ mbar.⁴⁰ Taking these pressures and the collision cross-section between intermediates **i1/i2** and a nitrogen bath molecule in Titan's atmosphere estimated as $0.61 \times 10^{-18} \text{ m}^{-2}$ (using textbook values for the collision cross-sections of benzene and N₂, 0.88×10^{-18} and $0.43 \times 10^{-18} \text{ m}^{-2}$, respectively), we obtain the time between collisions at $T = 90 \text{ K}$ as $\sim 70 \text{ ns}$ and 70 ms at 1 and 10⁻⁶ mbar, respectively. The calculated lifetime of **i1/i2** is in the range of 20–45 μs (see Table S2) and hence collisional stabilization would be possible at 1 mbar but not

at 10⁻⁶ mbar. More sophisticated RRKM/Master Equation (RRKM-ME) calculations of pressure and temperature dependent rate constants and product branching ratios would be required to determine the relative yield of the stabilized C₁₀H₉ intermediates, which is beyond the scope of the present paper. Meanwhile, an estimate of the likelihood of collisional stabilization of **i1/i2** can be made based on the recent RRKM-ME study of the C₆H₆ + C₂H reaction by Woon.⁴¹ According to his calculations, the relative yield of the stabilized C₆H₆C₂H adduct in the reaction of benzene with ethynyl radical exceeds 50% at pressures higher than 4.1, 11.5, 22.0, 39.9, 66.7, and 117.9 mbar at temperatures of 50, 100, 150, 200, 250, and

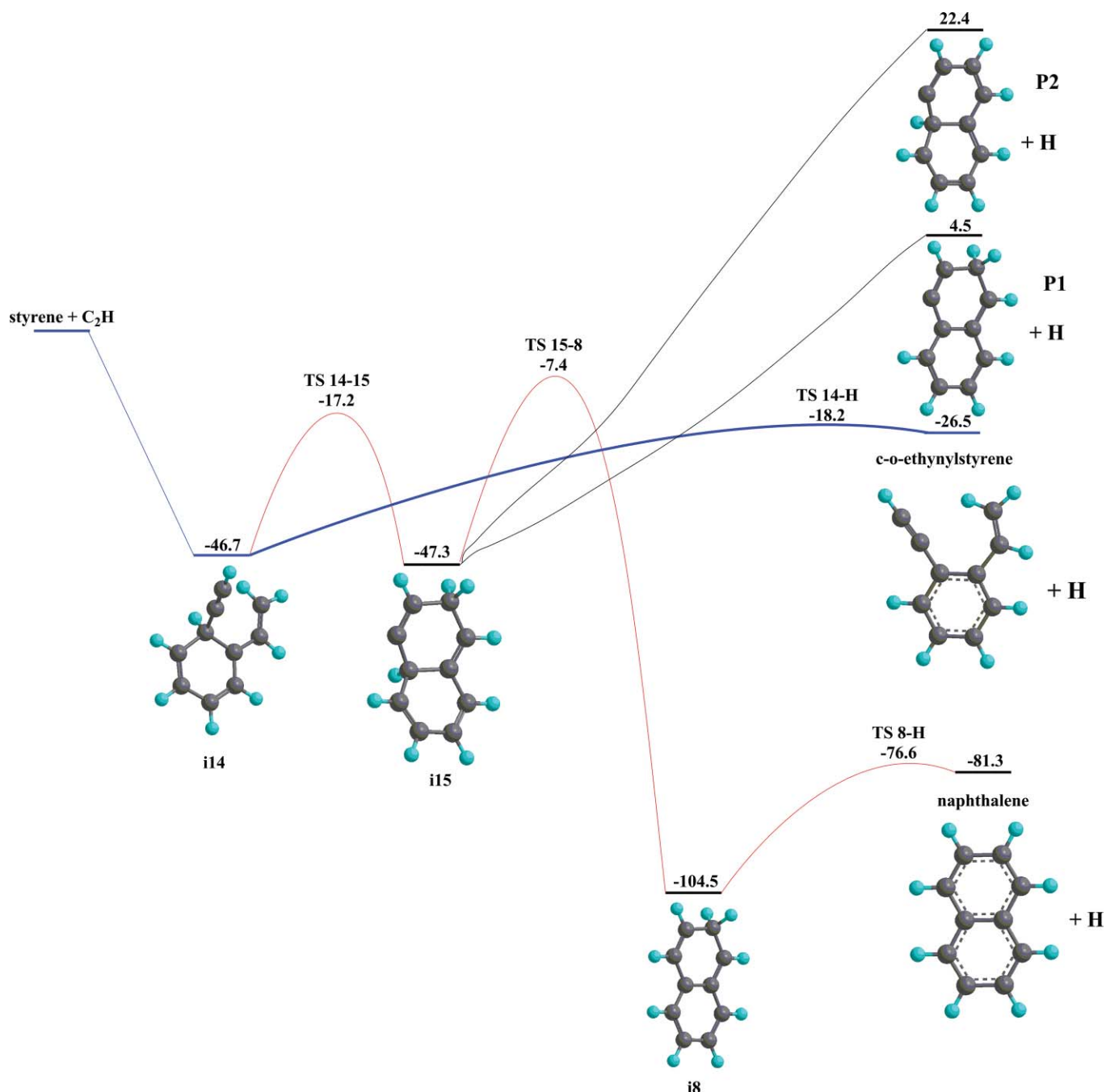


FIG. 2. Potential energy diagram of the styrene + C₂H reaction (channels initiated by the C₂H addition to the C⁶ atom in styrene) calculated at the G3(MP2,CC)//B3LYP/6-311G** + ZPE(B3LYP/6-311G**) level of theory. All relative energies are given in kcal/mol with respect to the initial reactants.

300 K, respectively. At the low pressures in Titan's haze-forming region and in the interstellar media, the yield of $C_6H_6C_2H$ is smaller than that of the $C_6H_5C_2H + H$ decomposition products, but a possibility of the adduct collisional stabilization in the range of 1–10% still exists at temperatures between 50 and 100 K at 1 mbar; the lower the temperature, the higher the yield of the stabilized radical adduct. Hence, the formation of a small amount of stabilized $C_{10}H_9$ radicals in the $C_2H +$ styrene reaction may occur under Titan's stratospheric conditions.

The second possible entrance channel for the styrene + C_2H reaction is the ethynyl attack in position 6 (see Fig. 2). This produces the initial adduct **i14** exothermic by 46.7 kcal/mol. At the next step, a loss of the hydrogen atom from the attacked C^6 carbon occurs via a barrier of 28.5 kcal/mol (at -18.2 kcal/mol relative to the reactants) and leads to the formation of *cis*-*o*-ethynylstyrene, which lies 26.5 kcal/mol lower in energy than styrene + C_2H . Alternatively, **i14** can be subjected to a ring closure involving a barrier of 29.5 kcal/mol (at -17.2 kcal/mol) to form **i15**, which is close in energy to **i14**. At this point, **i15** may undergo H loss from two different positions, the CH_2 group and the C atom in the C–C bond shared by the rings. However, both final H elimination products **P1** and **P2** are high in energy, 4.5 and 22.4 kcal/mol above the initial reactants, respectively, and hence are not likely to be formed to any appreciable extent. On the other hand, instead of the H loss, **i15** may experience an H shift to the hydrogen-less carbon atom leading to 2-hydronaphthyl radical **i8** via a barrier of 39.9 kcal/mol (at -7.4 kcal/mol). We already considered above that **i8** can eliminate a CH_2 hydrogen atom to produce naphthalene.

When C_2H adds to position 6 and **i14** serves as the initial adduct, the only observable product is expected to be *c*-*o*-ethynylstyrene (*cis*-1-ethenyl-2-ethynyl-benzene). The barrier for the H loss from **i14** is ~ 11 kcal/mol lower than the energy of the critical transition state TS15–8 relative to **i14** on the **i14** \rightarrow **i15** \rightarrow **i8** cyclization path. Therefore, the ring closure is unfavorable and naphthalene would not be formed. In the steady-state approximation, the rate constant for the production of naphthalene from **i14** is calculated as

$$\frac{k_{14-15}k_{15-8}k_{8-H}}{k_{15-14}k_{8-15} + k_{15-14}k_{8-H} + k_{15-8}k_{8-H}} \approx \frac{k_{14-15}}{k_{15-14}}k_{15-8}.$$

This simplification is possible because the **i15** \rightarrow **i8** is the rate-limiting step and, as a result, the $k_{15-14}k_{8-H}$ term is the largest in the denominator (see supplementary material). The $(k_{14-15}/k_{15-14})/k_{15-8}$ rate constant is 4–5 orders of magnitude lower than k_{14-H} for the direct H loss in **i14**.

By analogy, we can expect that C_2H addition to position 2 will produce a *trans* conformation of *o*-ethynylstyrene (*t*-*o*-ethynylstyrene or *trans*-1-ethenyl-2-ethynyl-benzene). In principle, C_2H can also add to the other positions in styrene (1, 3-5, and 7; see Scheme 1). However, in those cases the formation of a second ring is even more improbable. For instance, the addition to 3-5 positions is expected to produce various ethenyl-ethynyl-benzenes (*m*- and *p*-ethynylstyrenes) after direct H loss from the attacked carbon atom in the benzene ring. The addition to position 1 is likely to form ethynylbenzene + C_2H_3 . By comparing with the analogous

$C_2H + C_2H_4$ reaction,⁴² we can also anticipate that C_2H addition to position 7 may produce 1-ethynyl-1-phenyl-ethene + H or vinylacetylene + C_6H_5 . In lieu of this consideration, we can conclude that the $C_2H +$ styrene reaction would not produce naphthalene.

Nevertheless, our calculations show the formation of several unsaturated hydrocarbons containing an aromatic ring and side chains. One of them, *o*-ethynylstyrene, is particularly interesting. In 2005, Zwier *et al.*⁴³ investigated the isomerization energetics of *o*-ethynylstyrene and noted that the *cis* form is 2 kcal/mol less stable than its *trans* conformer. The authors suggested that if *cis*-ethynylstyrene can be formed, a cyclization process in combustion flames should be the most facile from of the *cis* conformer. It is worth noting that their spectroscopic measurements were only able to identify the *trans* conformer. It is, therefore, interesting that our electronic structure calculations show a direct route for the formation of the *cis* conformation of *o*-ethynylstyrene. Meanwhile, C_2H addition to position 2 in styrene is expected to produce the *trans* conformation. Electronic structure calculations by Prall *et al.* showed that the ring closure in *cis*-*o*-ethynylstyrene occurs through an activation barrier of 32.1 kcal/mol at the BLYP/6-31G* level of theory and subsequent H migrations may then lead to naphthalene.⁴⁴ In addition, through shocktube studies, Schulz *et al.* demonstrated that PVA can isomerize to naphthalene.⁴⁵ The processes discussed above occur at high temperatures and are not likely to be relevant to Titan's atmospheric chemistry. However, the products of the $C_2H +$ styrene reaction may be able to encounter a second C_2H unit and such $C_{10}H_8 + C_2H$ reactions are considered in the following section.

B. Addition of a second C_2H unit

Here, we consider C_2H reactions with most probable primary products of the styrene + C_2H reaction described above, including *trans* and *cis* phenylvinylacetylenes and *cis*-*o*-ethynylstyrene. It should be noted that these molecules contain several double, triple, and aromatic C–C bonds, and all of them can be subjected to a barrierless C_2H addition forming a great variety of initial adducts. However, in the present work we investigate only those channels, which can potentially lead to a second ring closure and formation of a PAH species.

An attack by the ethynyl radical toward the *ortho* ring carbon in **t-PVA** produces the initial adduct **i16**, which is stabilized by about 45 kcal/mol relative to the initial reactants (Fig. 3). At this point, **i16** can isomerize to **i17** via a 44.5 kcal/mol barrier corresponding to a 1,2-H shift from the ring to the C_2H side chain. Alternatively, a hydrogen atom can be lost from the attacked ring C atom in **i16** giving rise to the $C_6H_4(C_2H)(CHCHC_2H)$ product **P3**. This step proceeds through a 34.9 kcal/mol barrier and the overall exothermicity of the **t-PVA** + $C_2H \rightarrow$ **P3** + H reaction is 23.9 kcal/mol. Lastly, **i16** can undergo ring closure producing the bicyclic intermediate **i18** via a 34.5 kcal/mol activation barrier. Next, a hydrogen migration in **i18** leads to **i19**, which lies in a deep potential well, 98.1 kcal/mol below the reactants. A loss of the C_2H group from **i19** can then pro-

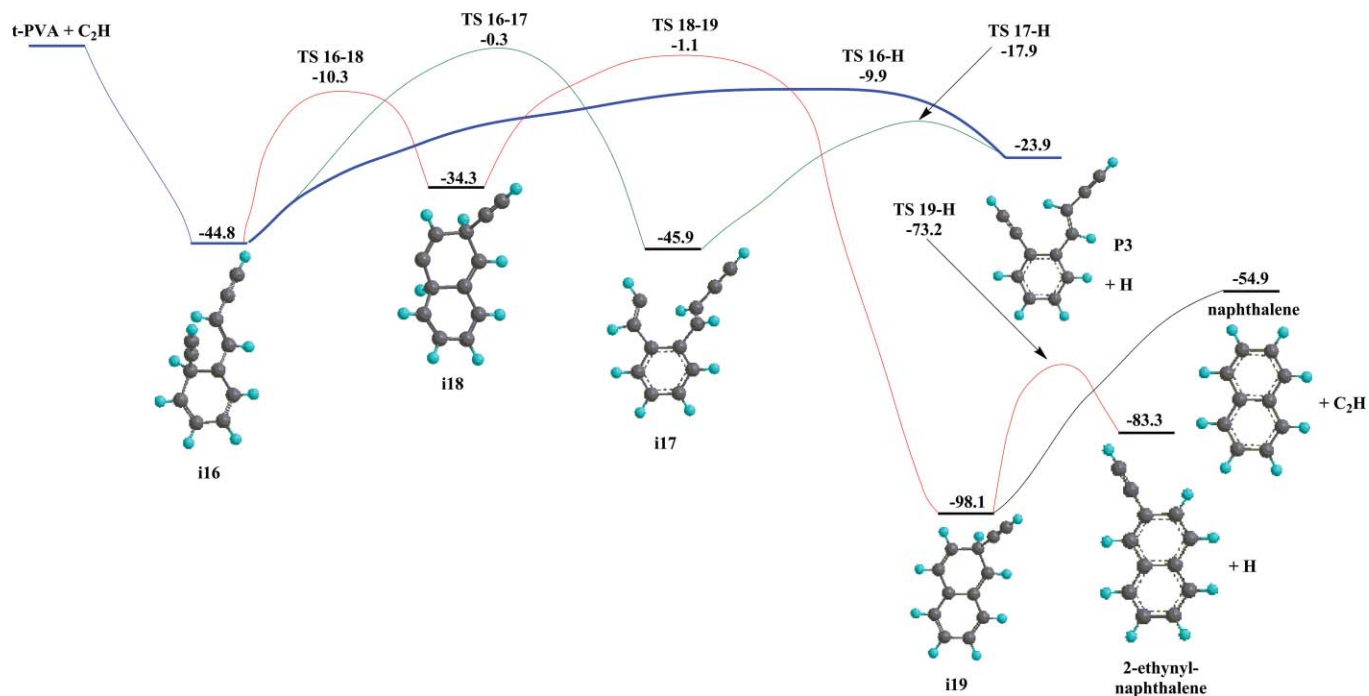


FIG. 3. Potential energy diagram of the **t-PVA** + C₂H reaction (channels initiated by the C₂H addition to the *ortho* carbon in the ring) calculated at the G3(MP2,CC)//B3LYP/6-311G** + ZPE(B3LYP/6-311G**) level of theory. All relative energies are given in kcal/mol with respect to the initial reactants.

duce naphthalene as the final product. This dissociation process occurs without an exit barrier and is endothermic by 43.2 kcal/mol. However, the alternative H loss from the tetrahedral carbon center in **i19** leading to 2-ethynyl-naphthalene is clearly more favorable, as it proceeds via a 24.9 kcal/mol barrier and is endothermic by only 14.8 kcal/mol. This area of the PES also illustrates that naphthalene can react with the ethynyl radical in a similar way as benzene, i.e., via the C₂H-for-H exchange mechanism. The C₂H addition to the second position in naphthalene is barrierless and exothermic by 43.2 kcal/mol (42.2 kcal/mol for benzene) and then H eliminations occurs from the attacked carbon atom via the barrier of 24.9 kcal/mol (24.4 kcal/mol in the case of benzene), with the overall C₂H + naphthalene → 2-ethynyl-naphthalene

+ H reaction being exothermic by 28.4 kcal/mol (the same as for benzene). Branching ratio calculations for the reaction scheme in Fig. 3 using our RRKM/kinetic equations approach show that **P3** + H should be the nearly exclusive product of the C₂H + **t-PVA** reaction under single-collision conditions when the ethynyl addition takes place to the *ortho* ring carbon. Indeed, the steady-state rate constant for the production of 2-ethynyl-naphthalene from **i16**,

$$\frac{k_{16-18}k_{18-19}k_{19-H}}{k_{18-16}k_{19-18} + k_{18-16}k_{19-H} + k_{18-19}k_{19-H}},$$

can be simplified as $(k_{16-18}/k_{18-16})/k_{18-19}$ because **i18** → **i19** is the rate-determining step making $k_{18-16}k_{19-H}$ the

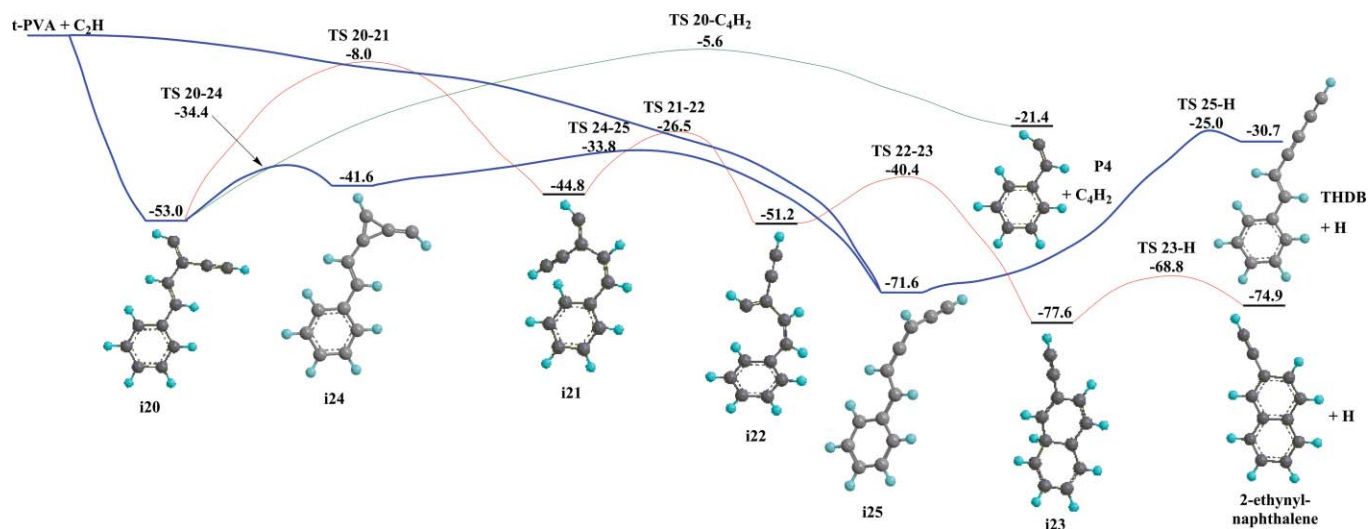


FIG. 4. Potential energy diagram of the **t-PVA** + C₂H reaction (channels initiated by α - and β -C₂H additions to the side chain) calculated at the G3(MP2,CC)//B3LYP/6-311G** + ZPE(B3LYP/6-311G**) level of theory. All relative energies are given in kcal/mol with respect to the initial reactants.

leading term in the denominator. This rate constant is ~ 5 orders of magnitude lower than k_{16-H} for the H elimination from **i16** to form **P3** + H.

C_2H addition can also occur to the triple bond carbons of the side chain in **t-PVA**. In particular, the ethynyl attack toward the β -C atom produces the intermediate **i20** with exothermicity of 53.0 kcal/mol (Fig. 4). The further fate of **i20** can be threefold. First, it can dissociate by losing a diacetylene fragment to produce C_6H_5CHCH **P4**. This C_4H_2 loss channel proceeds via a barrier of 47.4 kcal/mol and the products are exothermic by 21.4 kcal/mol. Second, two consequent rotations around C–C bonds in **i20** featuring barriers of 45.0 and 18.3 kcal/mol lead to the structure **i22** via **i21**. **i22** lies 51.2 kcal/mol below the initial reactants. Ring closure in this intermediate is facile, as it occurs via a barrier of 10.8 kcal/mol, and leads to the bicyclic intermediate **i23**, with a relative energy of -77.6 kcal/mol. Hydrogen loss can then occur with a 8.8 kcal/mol barrier to yield 2-ethynyl-naphthalene. The third competing pathway from **i20** features a two-step C_2H migration to the terminal carbon. The barriers for the first and second steps in this process are 18.6 and 7.8 kcal/mol, respectively, and the C_2H shift leads to the formation of **i25** via a bicyclic intermediate **i24**. **i25** can decompose by a loss of a hydrogen atom via a 46.6 kcal/mol barrier producing *trans*-1-hexene-3,5-diyne-benzene (**THDB**). The **THDB** + H products reside 30.7 kcal/mol below the C_2H + **t-PVA** reactants. **i25** can also be formed directly from the reactants by addition of the ethynyl radical to the α -C atom of the side chain. After that, this initial adduct can either dissociate to **THDB** + H or isomerize to **i20** via the C_2H migration described above.

Figure 5 illustrates various pathways of the C_2H + **c-PVA** reaction. For instance, ethynyl radical addition to the β -carbon in **c-PVA**'s side chain can directly lead to **i22**, thus avoiding the difficult steps involving the double bond rotations, which are required for its formation from the initial adduct **i20** in the C_2H + **t-PVA** reaction. As we already know, ring closure in **i22** gives **i23**, which can easily split a hydrogen to form 2-ethynyl-naphthalene. Alternatives to the cyclization process in **i22** include C_4H_2 elimination to produce **P4** and a two-step C_2H shift to form **i27**, analogous to the **i20** \rightarrow **i24** \rightarrow **i25** pathway. The intermediate **i27** also serves as the initial adduct in the C_2H + **c-PVA** reaction when the ethynyl radical attacks the α -C atom in **c-PVA**. For such α -addition, competing reaction scenarios include direct H loss from **i27** to form a *cis* conformation of HDB (**CHDB**) and isomerization to **i22** followed by either cyclization and H loss yielding 2-ethynyl-naphthalene or C_4H_2 elimination producing **P4**. In our RRKM calculations, we therefore considered four different possibilities including α - and β -additions of C_2H to **t-PVA** and **c-PVA**. The calculated branching ratios are presented in Table I. Based on the branching ratios, one can see that 2-ethynyl-naphthalene can only be formed starting from the *cis* isomer of **PVA**. The reaction with **t-PVA** appears to be incapable of forming the naphthalene core, because the cyclization process is hindered by the high barrier for the preceding *trans*-*cis* isomerization step **i20** \rightarrow **i21** involving rotation around a double C=C bond. On the other hand, the

initial adduct **i22** in the reaction with **c-PVA** is already in position to cyclize and, therefore, the double bond rotation can be avoided.

The branching ratio results can be also rationalized using the steady-state expressions for the rate constants (see supplementary material).³⁷ For the formation of **THDB** in the C_2H + **t-PVA** reaction (Fig. 4) from **i20**, the expression can be simplified as $(k_{20-24}/k_{24-20})(k_{24-25}/k_{25-24})k_{25-H}$ because the last H elimination step from **i25** is rate-controlling and a pre-equilibrium should be established for **i25**. For the formation of 2-ethynyl-naphthalene, the first step, **i20** \rightarrow **i21**, is rate-determining and hence the rate constant expression can be simplified as k_{20-21} . A comparison of $(k_{20-24}/k_{24-20})(k_{24-25}/k_{25-24})k_{25-H}$, k_{20-21} , and $k_{20-C_4H_2}$ values shows that the first one is several orders of magnitude higher than the second and the third, and thus the production of **THDB** is dominant among the reaction channels shown in Fig. 4. For the C_2H + **c-PVA** reaction, the simplified expressions for the rate constants to form **CHDB**, 2-ethynyl-naphthalene, and **P4** + C_4H_2 , respectively are $(k_{22-26}/k_{26-22})(k_{26-27}/k_{27-26})k_{27-H}$, k_{22-23} , and $k_{22-C_4H_2}$, and k_{22-23} has the highest value as it corresponds to the lowest barrier for transformations of **i22**. On the other hand, when **i27** is the initial intermediate the rate constant of **CHDB** formation is k_{27-H} , whereas that to produce 2-ethynyl-naphthalene via the multistep **i27** \rightarrow **i26** \rightarrow **i22** \rightarrow **i23** mechanism can be roughly estimated as $(k_{27-26}/k_{26-27})k_{26-22}$ because the **i26** \rightarrow **i27** step has the highest in energy transition state and the $k_{26-27}k_{22-23}k_{23-H}$ term is the largest in the denominator of the corresponding rate constant expression (see supplementary material).³⁷ In this case, the direct H loss from **i27** appears to be more favorable, although a significant amount of 2-ethynyl-naphthalene is also produced.

Now we consider C_2H additions to the ethynyl side chain in *c-o*-ethynylstyrene. The addition to the α -position occurs through a barrierless entrance channel producing **i28**, with an exothermicity of 65.0 kcal/mol (Fig. 6). A direct H loss from **i28** occurs via a 40.1 kcal/mol barrier and leads to the formation of 1-buta-1,3-diyne-2-vinyl-benzene (**BDVB**). **BDVB** lies 30.7 kcal/mol below the initial reactants. Alternatively, **i28** can isomerize to the most stable **i31** isomer, 107.8 kcal/mol below the reactants, via two different two-step pathways. Both of them involve ring closure and 1,2-hydrogen migration but these steps occur in different orders. In the first pathway, **i28** \rightarrow **i29** \rightarrow **i31**, the H shift takes place first and is followed by the cyclization, whereas in the second, **i28** \rightarrow **i30** \rightarrow **i31**, the sequence is reversed. In both channels, the highest barrier corresponds to the H migration steps and the respective transition states TS 28–29 and TS 30–31 are located 47.3 and 48.4 kcal/mol higher in energy than **i28**. **i31** can split a hydrogen atom from the CH_2 group to produce 2-ethynyl-naphthalene via a barrier of 28.8 kcal/mol. Alternatively, **i31** can be subjected to H migration from CH_2 over a potential barrier of 39.5 kcal/mol to form **i32** with a C(H)(C_2H) group. **i32** is an enantiomer of **i19** (Fig. 3) and it can either barrierlessly lose the C_2H group to form naphthalene with endothermicity of 44.4 kcal/mol, or expel the hydrogen atom from the *sp*³ carbon overcoming a lower barrier of 22.1

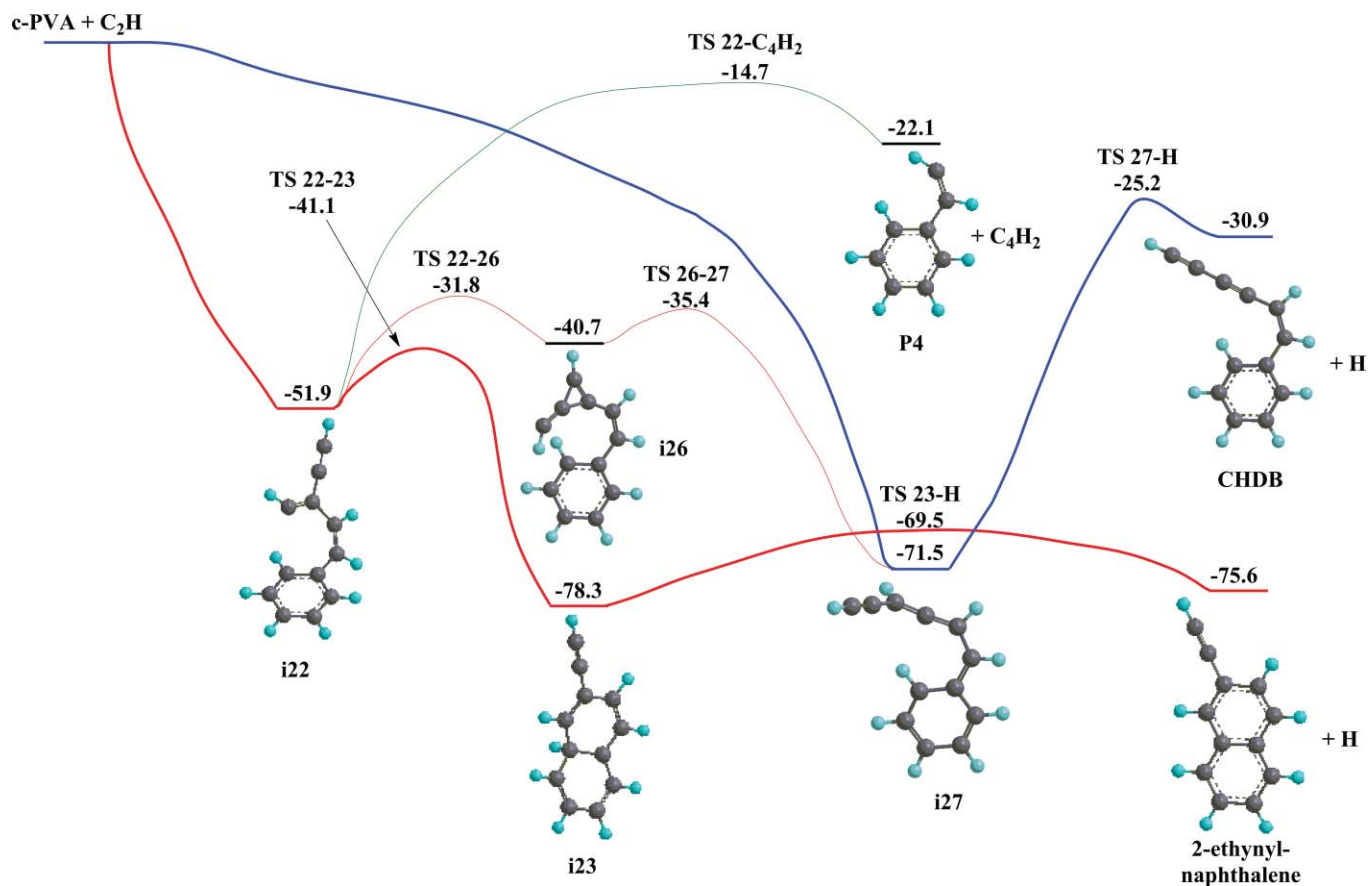


FIG. 5. Potential energy diagram of the *c*-PVA + C₂H reaction (channels initiated by α - and β -C₂H additions to the side chain) calculated at the G3(MP2,CC)//B3LYP/6-311G** + ZPE(B3LYP/6-311G**) level of theory. All relative energies are given in kcal/mol with respect to the initial reactants.

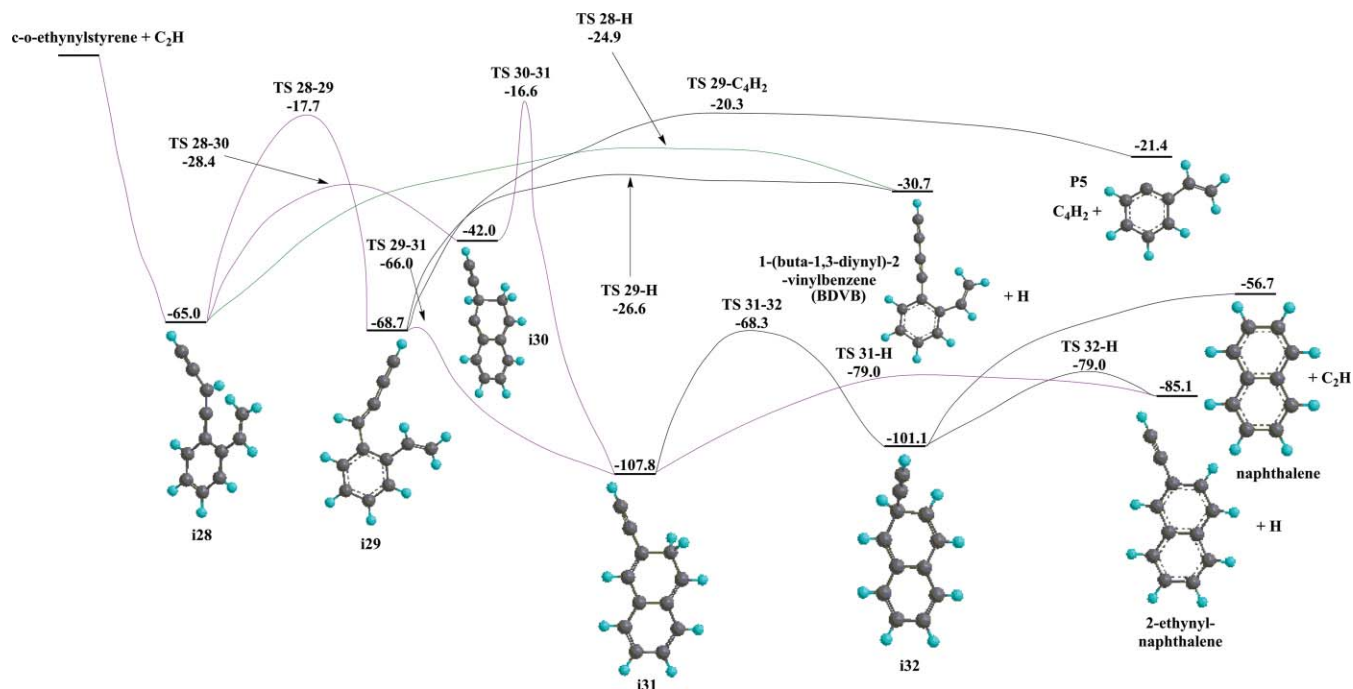


FIG. 6. Potential energy diagram of the *c*-*o*-ethynylstyrene + C₂H reaction (channel initiated by α -C₂H addition to the ethynyl side chain) calculated at the G3(MP2,CC)//B3LYP/6-311G** + ZPE(B3LYP/6-311G**) level of theory. All relative energies are given in kcal/mol with respect to the initial reactants.

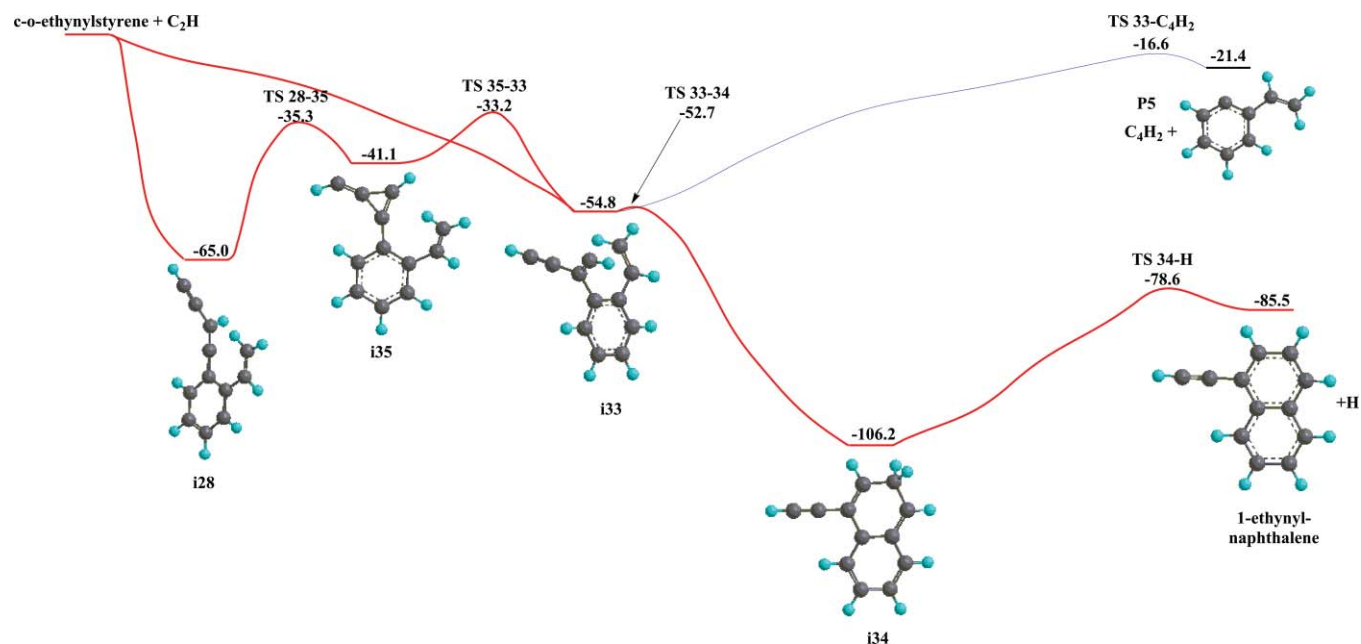


FIG. 7. Potential energy diagram of the *c-o*-ethynylstyrene + C₂H reaction (channel initiated by β -C₂H addition to the ethynyl side chain) calculated at the G3(MP2,CC)//B3LYP/6-311G** + ZPE(B3LYP/6-311G**) level of theory. All relative energies are given in kcal/mol with respect to the initial reactants.

kcal/mol to produce 2-ethynyl-naphthalene. To complete the description of all possible reaction channels shown in Fig. 6, we should mention decomposition pathways of **i29**, including H loss producing BDVB and C₄H₂ elimination giving rise to the C₆H₄C₂H₃ radical **P5**. However, both of these dissociation channels feature relatively high barriers of 42.1 and 48.4 kcal/mol, respectively, and hence they are not expected

to compete with **i29** → **i31** cyclization pathway occurring via a low 2.7 kcal/mol barrier.

Finally, C₂H can attack the β -position of the ethynyl side chain in *c-o*-ethynylstyrene producing adduct **i33** (see Fig. 7) with an energy gain of 54.8 kcal/mol. Once **i33** is produced, it can easily cyclize via a low 2.1 kcal/mole barrier forming **i34**. Next, a hydrogen loss from the latter gives 1-ethynyl-

TABLE I. Calculated branching of various C₂H + phenylvinylacetylene and C₂H + *c-o*-ethynylstyrene reactions at different collision energies under single-collision conditions.

Reactions and products	Collision energy (kcal/mol)					
	0.0	1.0	2.0	3.0	4.0	5.0
C₂H + t-PVA (Fig. 4, starting from i20 or i25)						
THDB + H	100	100	100	100	100	100
2-ethynyl-naphthalene + H	0	0	0	0	0	0
P4 + C ₄ H ₂	0	0	0	0	0	0
C₂H + c-PVA (Fig. 5, starting from i22)						
CHDB + H	4	4	4	5	5	5
2-ethynyl-naphthalene + H	96	96	96	95	95	95
P4 + C ₄ H ₂	0	0	0	0	0	0
C₂H + c-PVA (Fig. 5, starting from i27)						
CHDB + H	70	71	72	72	72	73
2-ethynyl-naphthalene + H	30	29	28	28	28	27
P4 + C ₄ H ₂	0	0	0	0	0	0
(C₂H + c-o-ethynylstyrene Figs. 6 and 7, starting from i28)						
BDVB + H	3.5	4.0	4.5	5.0	5.6	6.2
P5 + C ₄ H ₂	0	0	0	0	0	0
1-ethynyl-naphthalene + H	96.5	96	95.5	95.0	94.4	93.8
(C₂H + c-o-ethynylstyrene Figs. 6 and 7, starting from i33)						
BDVB + H	0	0	0	0	0	0
P5 + C ₄ H ₂	0	0	0	0	0	0
1-ethynyl-naphthalene + H	100	100	100	100	100	100

naphthalene as the final product overcoming a barrier of 27.6 kcal/mol. Alternatively, **i33** may lose diacetylene to form **P5** with an activation energy of 38.2 kcal/mol. The **i33** adduct can be also accessed from **i28**, which is the initial complex corresponding to the α -addition of C₂H to *c-o*-ethynylstyrene. **i28** can isomerize to **i33** via a two-step C₂H migration process, occurring via a bicyclic intermediate **i35** and featuring barriers of 29.7 and 7.9 kcal/mole for the first and second steps, respectively. The **i28** \rightarrow **i35** \rightarrow **i33** channel should be competitive to the other isomerization and dissociation pathways of **i28** illustrated in Fig. 6 and, conversely, the **i33** \rightarrow **i35** \rightarrow **i28** path followed by further changes of **i28** may in principle compete with the ring closure in **i32**. Therefore, in our kinetic calculations of product branching ratios we treated the two reaction schemes shown in Figs. 6 and 7 together, but took **i28** and **i33** as two different possible initial adducts. The results of RRKM calculations (see Table I) of individual rate constants followed by solving kinetic equations show that indeed the overwhelmingly major product is 1-ethynyl-naphthalene. Moreover, the branching ratios are fairly insensitive to which, of the two entrance channels, is pursued. Although the exact steady-state rate constant expressions for product formation are very complex and involve 7 \times 7 determinants (see supplementary material),³⁷ rough simplified equations can be written by finding a rate-determining step for each process and using pre-equilibrium approximation for all preceding steps (here we consider **i28** as the initial adduct):

$$k(1\text{-ethynyl-naphthalene}) \approx \frac{k_{28-35}}{k_{35-28}} k_{35-33}.$$

$$k(2\text{-ethynyl-naphthalene}) \approx k_{28-29}.$$

$$k(\text{BDVB}) \approx k_{28-H}.$$

$$k(\text{P5} + \text{C}_4\text{H}_2) \approx \frac{k_{28-35}}{k_{35-28}} \frac{k_{35-33}}{k_{33-35}} k_{33-\text{C}_4\text{H}_2}.$$

The use of these overly simple expressions qualitatively reproduces the product branching ratios obtained from the exact solution.

Although our mechanism starts with C₂H addition to the *cis* isomer of *o*-ethynylstyrene, we show in Fig. 8 that *t-o*-ethynylstyrene observed experimentally is just as likely to proceed toward the formation of the naphthalene core after an encounter with the ethynyl radical. C₂H addition to the *trans* isomer leads to the formation of isomer **t-i28** and its rearrangement to the *cis* isomer **i28** occurs with only a 3.2 kcal/mol barrier. This means that the *trans* adduct can be also converted quickly and efficiently to 1-ethynyl-naphthalene.

C. Prospects for further PAH growth

While the reactions of two consecutive C₂H additions to styrene considered in this study are not likely to produce naphthalene itself, they appear to be a potential source for the formation of substituted naphthalene derivatives. For instance, C₂H additions to the side chain of *cis* phenylvinyl-

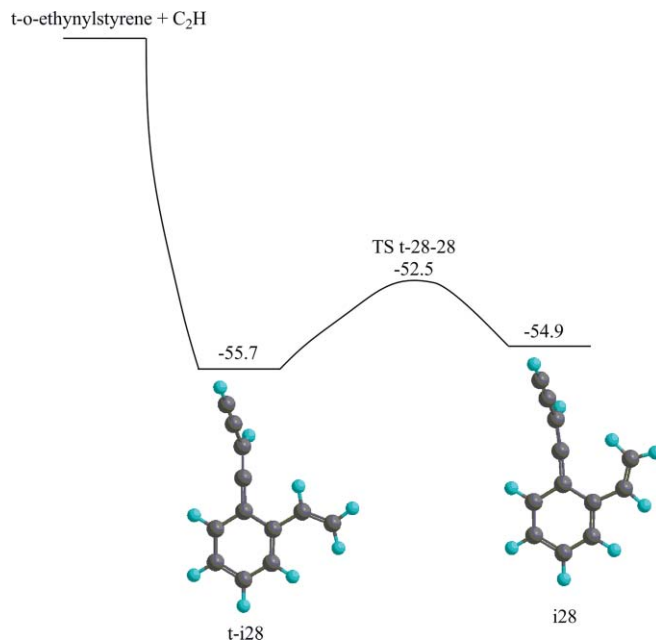


FIG. 8. Potential energy diagram of the initial steps in the *t-o*-ethynylstyrene + C₂H reaction (channel initiated by α -C₂H addition to the ethynyl side chain) calculated at the G3(MP2,CC)//B3LYP/6-311G** + ZPE(B3LYP/6-311G**) level of theory. All relative energies are given in kcal/mol with respect to the initial reactants.

lacetylene can synthesize 2-ethynyl-naphthalene with the branching ratios of 96% and 30% for the β and α addition, respectively, at zero collision energy. Also, the ethynyl side chain addition of C₂H to *o*-ethynylstyrene is predicted to nearly exclusively form 1-ethynyl-naphthalene. This mechanism offers the advantage of producing fully closed-shell molecules with the naphthalene core and, therefore, represents an overall improvement over the EAM mechanism suggested earlier and involving C₂H additions to benzene, ethynylbenzene, etc., where only naphthyl radical and didehydronaphthalene derivatives can be formed. The possibilities for further PAH growth starting from either 1-ethynyl-naphthalene or 2-ethynyl-naphthalene are numerous. For example, on the course of EAM, the addition of C₂H to the *ortho* position (with respect to the ethynyl group) of 1-ethynyl-naphthalene, followed by H-loss, second C₂H addition, and cyclization will lead to derivatives of phenanthryl radical and didehydrophenanthrene. Similarly, C₂H additions to the *ortho* positions of 2-ethynyl-naphthalene can eventually lead to either phenanthryl radical and didehydrophenanthrene or anthracyl radical and didehydroanthracene derivatives. If a PAH molecule contains an out-of-ring vinyl group (a larger homologue of styrene), it may undergo two consecutive C₂H additions analogous to the reactions described in this study, resulting in the formation of an additional ring in the polycyclic aromatic system. It is also noteworthy to point out that if the ethynyl additions in the proposed mechanisms are replaced by barrierless additions of the cyano (CN) radical and/or if the initial reactant is methyleneamino-benzene (methyleneamino-PAH) instead of styrene (vinyl-PAH), similar reactions may lead to the formation of nitrogen containing polycyclic aromatic compounds (N-PACS),⁴⁶ which are also believed to be important molecular constituents of Titan's organic hazes.

IV. CONCLUSION

We have investigated several mechanisms of the formation of naphthalene and its substituted derivatives by studying potential energy surfaces for the reactions of one and two C_2H additions to styrene. For the first ethynyl addition, $C_2H + \text{styrene}$, despite that various reaction channels may lead to a second ring closure and the production of naphthalene, the dominant route in all mechanisms considered appears to be H atom elimination from the initial adduct. For instance, C_2H addition to the vinyl side chain of styrene is predicted to produce *trans* or *cis* conformations of phenylvinylacetylene, **t**- and **c**-PVA, whereas C_2H addition to the *ortho* carbon in the ring is expected to lead to the formation of *o*-ethynylstyrene. However, both phenylvinylacetylene and *o*-ethynylstyrene may undergo a second addition of the ethynyl radical to ultimately produce substituted naphthalene derivatives. In particular, α - and β -additions of C_2H to the side chain in **c**-PVA are calculated to proceed by the following mechanism, $C_2H + \text{c-PVA} \rightarrow (\mathbf{i27} \rightarrow \mathbf{i26} \rightarrow) \mathbf{i22} \rightarrow \text{ring closure} \rightarrow \mathbf{i23} \rightarrow \text{H loss} \rightarrow 2\text{-ethynyl-naphthalene} + \text{H}$, and are predicted to form 2-ethynyl-naphthalene with branching ratios of about 30% and 96%, respectively; in the case of α -addition the major product would be *cis*-1-hexene-3,5-diynyl-benzene (**CHDB**) produced by an immediate H elimination from the initial adduct **i27**. C_2H addition to the ethynyl side chain in *o*-ethynylstyrene (regardless of α - or β -position of the attacked C atom) is predicted to lead to the formation of 1-ethynyl-naphthalene as a major or nearly exclusive product by the following mechanism: $C_2H + o\text{-ethynylstyrene} \rightarrow (\mathbf{i28} \rightarrow \mathbf{i35} \rightarrow) \mathbf{i33} \rightarrow \text{ring closure} \rightarrow \mathbf{i34} \rightarrow \text{H loss} \rightarrow 1\text{-ethynyl-naphthalene} + \text{H}$. The reactions considered here, $C_2H + \text{styrene} \rightarrow \text{t-PVA} + \text{H} / \text{c-PVA} + \text{H} / o\text{-ethynylstyrene}$, $C_2H + \text{c-PVA} \rightarrow 2\text{-ethynyl-naphthalene} + \text{H}$, and $C_2H + o\text{-ethynylstyrene} \rightarrow 1\text{-ethynyl-naphthalene} + \text{H}$, are predicted to occur without a barrier and with high exothermicity, with all intermediates, transition states, and products lying significantly lower in energy than the initial reactants. By the analogy with C_2H reactions with alkynes, alkenes, and aromatic benzene,²⁰ both first and second C_2H addition to styrene is expected to be fast, with rate constants on the order of $10^{-10} \text{ cm}^3 \text{ molecule}^{-1} \text{ s}^{-1}$, even at very low temperature conditions prevailing in Titan's atmosphere or in the interstellar medium. Therefore, once styrene and C_2H are available (the latter can be formed by photodissociation of acetylene at photon wavelengths below 217 nm) and overlap in such conditions, the sequence of two C_2H additions can result in the closure of a second aromatic ring and the formation of 1- or 2-ethynyl-naphthalene. The analogous mechanism can be extrapolated to the low-temperature growth of polycyclic aromatic hydrocarbons in general, from a vinyl-PAH to an ethynyl-substituted PAH with an extra aromatic ring.

Experimental verification of the suggested mechanism will require two stages. First, one needs to demonstrate that the $C_2H + \text{styrene}$ reaction can indeed produce phenylvinylacetylene and *o*-ethynylstyrene. Since these and other possible $C_{10}H_8$ products (such as various *m*- and *p*-ethynylstyrenes) are expected to be rather close in energy,

their identification will apparently require the use of spectroscopic techniques beyond the time-of-flight mass spectrometry utilized for universal product detection in crossed molecular beams experiments. Second, crossed molecular beams measurements of the $C_2H + o\text{-ethynylstyrene}$ and $C_2H + \text{cis-phenylvinylacetylene}$ reactions (if the *cis* conformer can be somehow isolated or produced in a beam) with the universal detection may allow for identification of 1- or 2-ethynyl-naphthalene as the products, because their energies are sharply distinct from the energies of other potential nonpolycyclic products. Since both *o*-ethynylstyrene and phenylvinylacetylene are commercially available⁴⁷ and their laboratory syntheses have been reported in the literature,^{43,48–50} we hope that the proposed experiments can be performed in the near future.

ACKNOWLEDGMENTS

This work was funded by the Collaborative Research in Chemistry (CRC) Program of the National Science Foundation (Award No. CHE-0627854).

- D. J. Cook, S. Schlemmer, N. Balucani, D. R. Wagner, B. Steiner, and R. J. Saykally, *Nature (London)* **380**, 227 (1996).
- L. J. Allamandola, A. G. G. M. Tielens, and J. R. Barker, *Astrophys. J., Suppl. Ser.* **71**, 733 (1989).
- E. Peeters, A. L. Mattioda, D. M. Hudgins, and L. J. Allamandola, *Astrophys. J.* **617**, L65 (2004).
- T. H. Jarrett, M. Polletta, I. P. Fournon, G. Stacey, K. Xu, B. Siana, D. Farrah, S. Berta, E. Hatziminaoglou, G. Rodighiero, J. Surace, D. Dominiq, D. Shupe, F. Fang, C. Lonsdale, S. Oliver, M. Rowan-Robinson, G. Smith, T. Babbedge, E. Gonzalez-Solares, F. Masci, A. Franceschini, and D. Padgett, *Astron. J.* **131**, 261 (2006).
- C. Sagan, W. R. Thompson, and B. N. Khare, *Acc. Chem. Res.* **25**, 286 (1992).
- B. N. Khare, C. Sagan, W. R. Thompson, E. T. Arakawa, F. Suits, T. A. Callcott, M. W. Williams, S. Shrader, H. Ogino, T. O. Willingham, and B. Nagy, *Adv. Space Res.* **4**, 59 (1984).
- C. Sagan, B. N. Khare, W. R. Thompson, G. D. McDonald, M. R. Wing, J. L. Bada, T. Vo-Dinh, and E. T. Arakawa, *Astrophys. J.* **414**, 399 (1993).
- B. N. Khare, N. Bishun, E. L. O. Bakes, H. Imanaka, C. P. McKay, D. P. Cruikshank, and E. T. Arakawa, *Icarus* **160**, 172 (2002).
- A. Coustenis, A. Salama, B. Schulz, S. Ott, E. Lellouch, Th. Encrenaz, D. Gautier, and H. Feuchtgruber, *Icarus* **161**, 383 (2003).
- A. Coustenis, R. K. Achterberg, B. J. Conrath, D. E. Jennings, A. Marten, D. Gautier, C. A. Nixon, F. M. Flasar, N. A. Teanby, B. Bezard, R. E. Samuelson, R. C. Carlson, E. Lellouch, G. L. Bjoraker, P. N. Romani, F. W. Taylor, P. G. J. Irwin, T. Fouchet, A. Hubert, G. S. Orton, V. G. Kunde, S. Vinatier, J. Mondlioni, M. M. Abvas, and R. Courtin, *Icarus* **189**, 35 (2007).
- M. McGuigan, J. H. Waite, H. Imanaka, and R. D. Sacks, *J. Chromatogr. A* **1132**, 280 (2006).
- M. Frenklach, *Phys. Chem. Chem. Phys.* **4**, 2028 (2002).
- J. D. Bittner and J. B. Howard, *Symp. (Int.) Combust., [Proc.]* **18**, 1105 (1981).
- H. Wang and M. Frenklach, *Combust. Flame* **110**, 173 (1997).
- E. H. Wilson and S. K. Atreya, *Planet. Space Sci.* **51**, 1017 (2003).
- E. H. Wilson, S. K. Atreya, and A. Coustenis, *J. Geophys. Res.* **108**, 5014 (2003).
- E. H. Wilson, and S. K. Atreya, *J. Geophys. Res.* **105**, 20263 (2000).
- A. M. Mebel, V.V. Kislov, and R. I. Kaiser, *J. Am. Chem. Soc.* **130**, 13618 (2008).
- D. Carty, V. LePage, I. R. Sims, and I. W. M. Smith, *Chem. Phys. Lett.* **344**, 310 (2001).
- E. Hebard, M. Dobrijevic, P. Pernot, N. Carrasco, A. Bergeat, K. M. Hickson, A. Canosa, S. D. Le Picard, and I. R. Sims, *J. Phys. Chem. A* **113**, 11227 (2009), and references therein.

- ²¹C. Berteloite, S. D. Le Picard, N. Balucani, A. Canosa, and I. R. Sims, *Phys. Chem. Chem. Phys.* **12**, 3666 (2010); *ibid.* **12**, 3677 (2010).
- ²²A. Landera, S. P. Krishtal, V. V. Kislov, A. M. Mebel, and R. I. Kaiser, *J. Chem. Phys.* **128**, 214301 (2008).
- ²³X. Gu, Y. S. Kim, R. I. Kaiser, A. M. Mebel, M. C. Liang, and Y. L. Yung, *Proc. Natl. Acad. Sci.* **106**, 16078 (2009).
- ²⁴W. M. Jackson and A. Scodinu, *Astrophys. Space Sci. Lib.* **31**, 1 85 (2004).
- ²⁵K. Seki and H. Okabe, *J. Phys. Chem.* **97**, 5284 (1993).
- ²⁶B. A. Balko, J. Zhang, and Y. T. Lee, *J. Chem. Phys.* **94**, 7958 (1991).
- ²⁷A. Läuter, K. S. Lee, K. H. Jung, R. K. Vatsa, J. P. Mittal, and H.-R. Volpp, *Chem. Phys. Lett.* **358**, 314 (2002).
- ²⁸M. C. Pietrogrande, P. Coll, R. Sternberg, C. Szopa, R. Navarro-Gonzalez, C. Vidal-Madjar, and F. Dondi, *J. Chromatogr. A* **939**, 69 (2001).
- ²⁹S. I. Ramirez, R. Navarro-Gonzalez, P. Coll, and F. Raulin, *Adv. Space Res.* **27**, 261 (2001).
- ³⁰F. Zhang, X. Gu, and R. I. Kaiser, *J. Org. Chem.* **72**, 7597 (2007).
- ³¹A. D. Becke, *J. Chem. Phys.* **98**, 5648 (1993); C. Lee, W. Yang, and R. G. Parr, *Phys. Rev. B* **37**, 785 (1988).
- ³²A. G. Baboul, L. A. Curtiss, P. C. Redfern, and K. Raghavachari, *J. Chem. Phys.* **110**, 7650 (1999); L. A. Curtiss, K. Raghavachari, P. C. Redfern, A. G. Baboul, and J. A. Pople, *Chem. Phys. Lett.* **314**, 101 (1999).
- ³³L. A. Curtiss, K. Raghavachari, P. C. Redfern, V. Rassolov, and J. A. Pople, *J. Chem. Phys.* **109**, 7764 (1998).
- ³⁴M. J. Frisch, G. W. Trucks, H. B. Schlegel *et al.*, GAUSSIAN 98, Revision A.11 Gaussian, Inc., Pittsburgh, PA, 1998.
- ³⁵M. J. Frisch, G. W. Trucks, H. B. Schlegel *et al.*, GAUSSIAN 09, Revision A.1 Gaussian, Inc., Wallingford, CT, 2009.
- ³⁶MOLPRO, a package of *ab initio* designed by H. J. Werner and P. J. Knowles, version 2002.6, R. D. Amos, A. Bernhardsson, A. Berning *et al.*
- ³⁷See supplementary material at <http://dx.doi.org/10.1063/1.3526957> for optimized Cartesian coordinates, energetic, and molecular parameters, including rotational constants and vibrational frequencies, of various structures (Table S1) and RRKM calculated rate constants of various unimolecular reactions (Table S2).
- ³⁸P. J. Robinson and K. A. Holbrook, *Unimolecular Reactions* (Wiley, New York, 1972); H. Eyring, S. H. Lin, and S. M. Lin, *Basic Chemical Kinetics* (Wiley, New York, 1980); J. Steinfield, J. Francisco, and W. Hase, *Chemical Kinetics and Dynamics* (Prentice Hall, Englewood Cliffs, NJ, 1989).
- ³⁹V. V. Kislov, T. L. Nguyen, A. M. Mebel, S. H. Lin, and S. C. Smith, *J. Chem. Phys.* **120**, 7008 (2004).
- ⁴⁰M. C. Liang, Y. L. Yung, and D. E. Shemansky, *Astrophys. J. Lett.* **661**, L199 (2007).
- ⁴¹D. E. Woon, *Chem. Phys.* **331**, 67 (2006).
- ⁴²S. P. Krishtal, A. M. Mebel, and R. I. Kaiser, *J. Phys. Chem. A* **113**, 11112 (2009); F. T. Zhang, Y. S. Kim, R. I. Kaiser, S. P. Krishtal, and A. M. Mebel, *J. Phys. Chem. A* **113**, 11167 (2009).
- ⁴³T. M. Selby, J. R. Clarkson, D. Mitchell, J. A. J. Fitzpatrick, H. D. Lee, D. W. Pratt, and T. S. Zwieter, *J. Phys. Chem. A* **109**, 4484 (2005).
- ⁴⁴M. Prall, A. Kruger, P. R. Schreiner, and H. Hopf, *Chem. Eur. J.* **7**, 4386 (2001).
- ⁴⁵K. Schulz, J. Hofmann, and G. Zimmermann, *Liebigs Ann./Recueil* **12**, 2535 (1997).
- ⁴⁶A. Landera and A. M. Mebel, *Faraday Disc.* **147**, 479 (2010).
- ⁴⁷Atomax Chemicals Product List; <http://www.atomaxchem.com>, Registry Numbers: 90766-20-4 and 13633-26-6.
- ⁴⁸K. M. Miller, T. Luanphaisarnnont, C. Molinaro, and T. F. Jamison, *J. Am. Chem. Soc.* **126**, 4130 (2004).
- ⁴⁹B. Kang, D. Kim, Y. Do, and S. Chang, *Org. Lett.* **5**, 3041 (2003).
- ⁵⁰W. Shen, and L. Wang, *J. Org. Chem.* **64**, 8873 (1999).